iJRASET
International Journal For Research in Applied Science and Engineering Technology

INTERNATIONAL JOURNAL FOR RESEARCH

IN APPLIED SCIENCE & ENGINEERING TECHNOLOGY

Volume: 6 **Issue:** II **Month of publication:** February 2018

DOI:

www.ijraset.com

Call: 08813907089 | E-mail ID: ijraset@gmail.com

International Journal for Research in Applied Science & Engineering Technology (IJRASET)
ISSN: 2321-9653; IC Value: 45.98; SJ Impact Factor: 6.887
Volume 6 Issue II, Feburary2018- Available at www.ijraset.com

Deformation and Analysis of AL6063/SIC/FlyAsh Hybrid Composites

Syed Feroz[1], N. Amara Nageswara Rao[2], Kakarla Sridhar[3]
[1]*Department of Mechanical Engineering, Nimra College Of Engineering And Technology, Ibrahim Patanam, Vijayawada, India*
[2]*Assosiate Professor, Department Of Mechanical Engineering, Nimra College Of Engineering Technology, Ibrahim Patanam, Vijayawada, India*
[3]*Hod & Prof Department Of Mechanical Engineering, Mvr College Of Engineering And Technology Vijayawada, India*

Abstract: ***There has been an increasing interest in composites containing low density and low cost reinforcements. So far most of the research work have been carried out by incorporating hard ceramic particles such as Al_2O_3, SiC, Flyash and graphite particles to soft matrix like pure aluminum, A2024, A356, A6063 and many more alloys and very few worked on combination of reinforcements (hybrid composites). In the current work, an attempt has been made by combining two types of ceramic particles like flyash and silicon carbide in equal proportions for preparation of hybrid composites, which significantly improves the mechanical properties and wear properties of the Aluminum based MMCs.***
Keywords: Al6063, SIC/FLY ASH, SCANNING ELECTRON MICROSCOPE

I. INTRODUCTION

Metal Matrix composites (MMCs) are becoming attractive materials for advanced aerospace and automobile structures because of their properties can be tailored through the addition of selected reinforcements [1, 2]. In particular particle reinforced MMCs have found special interest because of their high specific strength and specific stiffness at room or elevated temperature. Normally micron sized ceramic particles are used as reinforcement to improve the properties of the MMCs. Ceramic particles have low coefficient of thermal expansion (CTE) than metallic alloys, and therefore incorporation of the these ceramic particles may exist interfacial mismatch between matrix and reinforcement. This phenomenon may be higher for high ceramic particle concentration. Among various dispersoids used, fly ash is one of the most inexpensive and low density reinforcement available in large quantities as solid waste by-product during combustion of coal in thermal power plants. Fly ash particles are classified into two types, precipitator and cenosphere. Initial investigations were made with process development using fiber reinforcement. Anisotropy, expensive fabrication cost and restricted secondary processing has led to the use of short fiber / particulate / whisker reinforced composites. The combination of good transverse properties, low cost high workability and significant increase in performance over unreinforced alloys are the commercially attractive features of these discontinuous reinforced composites. Compared to dispersion strengthened systems, particulate reinforced composites contain coarse size reinforcement (1-99 μm) in relatively high weight fractions (1-40%). In particulate composites, both matrix and reinforcement bear substantial load. In addition, matrix strength as affected by precipitation and dislocation strengthening plays an important role in the load bearing capacity of these composites. Metal matrix composites reinforced with ceramic particles are widely used due to their high specific modulus, strength and wear resistance.

II. METHODS

A. *Fabrication Facilities*

1) *Furnace:* In the present investigation, preparation of alloys and fabrication of composites were carried out in pot furnace, furnace details were given below.

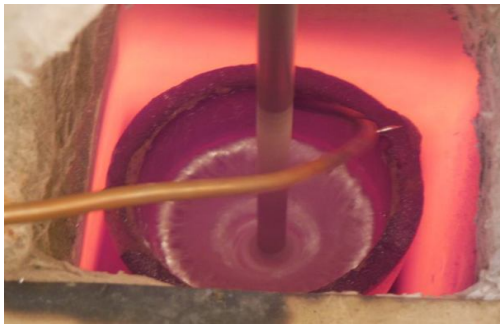

Figure (a) Pot Furnace, (b) same with a stirrer

2) *Furnace Details:* The following are the furnace details for preparation of alloys and fabrication of composites and process details were discussed thoroughly.

Furnace	:	Pot furnace
Make	:	KRISHMET-T
Heating element	:	KANTHAL-A1
Melt capacity	:	1.6 kg.

B. Testing Facilities

1) Physical Testing

a) Optical Microscopy: Standard polishing techniques were used to study the microstructures. Dilute Keller's reagent was used for etching. Study of microstructures and recording was done using Olympus, C – 5060- G x 4, Japan, shown in figure 2.2.

Composition of Keller's reagent: HF= 1.0 cc, HCL =1.5 cc, HNO_3 =2.5 cc H_2O= 95cc

Figure 3.2 Set up of Image Analyzer (Olympus, C – 5060 – G x 4 Japan)

SEM & EDS

Scanning electron microscopy (SEM) and Energy Dispersive X-ray Spectroscopy (EDS) were carried out using SEM-Hitachi S-3400N – Japan and SEM – ZEISS SUPRA 55VP operated at 20 kV, in order to evaluate the morphological and chemical compositions observed in the present investigation.

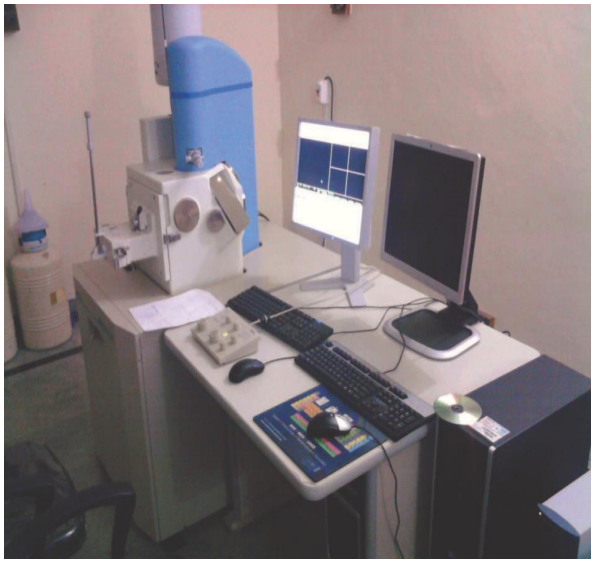

Figure 3.3 Scanning Electron Microscope (ZEISS SUPRA55VP)

b) Maintaining the Integrity of the Specifications XRD: All the investigated alloy powders was characterized with an X-Ray Diffractometer figure 2.4 (Model: 2036E201; Rigaku, Ultima IV, Japan). JADE software was used to investigate the phases present in them. Sample preparation of XRD was done as per the standard practice. The X-ray diffraction measurements were carried out with the help of a Goniometer model 2036E201 using Cu K radiation (K = 1.56056 A^0) at an accelerating voltage of 40 kV and a current of 20 mA. In this test the sample was in stationary condition, only the arms of the X- ray tube was rotating in the opposite direction up to 90 ^{0} of 2 during the test. The samples were scanned in the range from 3^0 to 90^0 of 2 with a scan rate of 2 ^{0}/ min.

Figure 3.4 X-ray diffraction Machine (Model: RIGAKU, ULTIMA-IV H-12-JAPAN)

III. MECHANICAL TESTING

A. Hardness

Vickers hardness studies were carried out for the investigated materials using micro Vickers micro hardness tester (Banbros (Model: LV 700) Hardness tester) with 1kg load. The indentation time for the hardness measurement was 15 seconds. An average of six readings were taken for each hardness value.

Figure 3.5 Banbros (Model: LV 700) Hardness tester

B. Tensile and compression

Tensile strength and compression strength of alloy and composites at room temperature was determined using a computer controlled 100kN DAK universal testing machine. Compression tests were carried out on cylindrical specimens. These cylindrical specimens of standard dimensions were prepared using conventional machining operations of turning and facing. Specimen edges were chamfered to minimize folding. Concentric v- grooves of 0.5mm deep were made on the flat surfaces to have a low friction between die and work piece during compression. Standard specimens of sizes Ø 12mm×12mm (H_o/D_o=1.0) and

Ø 18mm×12mm (H_o/D_o= 1.5) are upset by placing between the flat platens at a constant cross head speed of 0.3mm/min in dry conditions.

S. No	Item	Description
1	Make	Dak system Inc
2	Model	9103
3	Capacity	150 kN
4	Platens	Die Steel
5	Diameter of the platens	120mm

Table 2.2 Compression testing machine details

Table 23 Uniaxial comparession test conditions

S.No	Control parameter	Value
1	Pre Load	0.03 KN
2	Safe Load	400 KN
3	Hold Time	80 sec
4	Load Rate	50 kN/Min
5	Stress Rate	15kN/Min
6	Strain Rate	0.002
7	Initial valve open	30%

IV. EXPERIMENTAL DETAILS

A. Ring Compression Test

In this test, a flat ring having geometry; outer diameter: inner diameter: height in proportions of 6:3:2; was upset plastically between two flat platens. shows the ring compression sample with OD: ID: H = 15:7.5:5 mm (6: 3: 2). These ring samples were allowed to deform slowly up to 50% at the rate of 0.25 mm/sec by using computer controlled electrical screw driven 100 kN universal testing machine (Model: UT 9102; Dak System Inc). The internal diameter of the ring was measured intermittently by stopping the test up to a maximum deformation of 50% or up to fracture whichever is earlier. As the height is reduced, the ring expands radially outwards. By measuring the change in specimen's internal diameter and using the curves which are obtained through theoretical analysis, the coefficient of friction was determined.

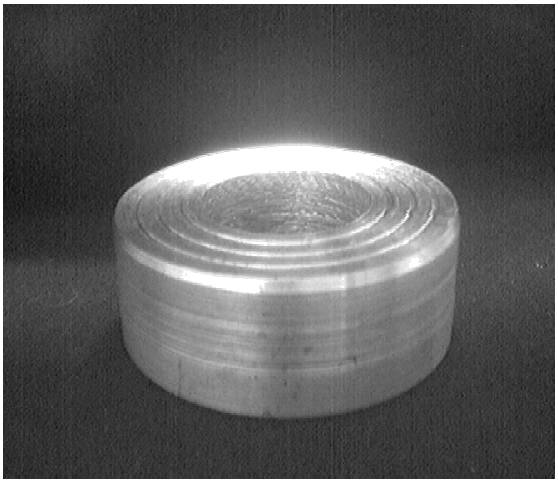

Figure Ring compression specimen (OD: ID: H = 6:3:2)

B. True Stress and True Strain

In metal working processes the work piece undergoes appreciable change in cross sectional area. Thus measures of stress and strain which are based on the instantaneous dimensions are needed. The engineering stress-strain curve does not give a true indication of the deformation characteristics of a material because it is based entirely on the original dimensions of the specimen and these dimensions change continuously during the test.

C. Engineering Stress and Engineering Strain

The engineering strain *e* is the ratio of the change in length to the original length [2-4].

$$e = \frac{\Delta L}{L_0} = \frac{L - L_0}{L_0} = \frac{1}{L_0}\int_{L_0}^{L} dL \text{---------- (1)}$$

$$\text{The engineering stress, } S = \frac{P}{A} \text{ ---------- (2)2)}$$

Ludwik [5] first proposed the definition of true strain or natural strain "". In this definition of strain the change in length is referred to the instantaneous gauge length, rather than to the original gage length

$$\varepsilon = \int_{L_0}^{L} \frac{dL}{L} = \ln\frac{L}{L_0} \text{ ---------- (3)}$$

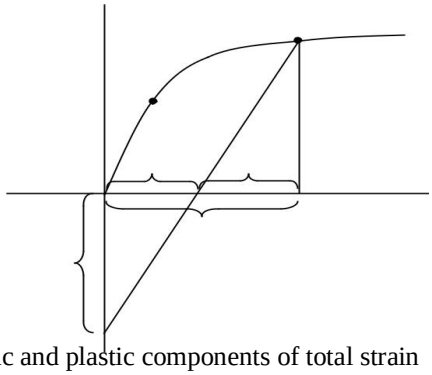

Figure 5.2 Elastic and plastic components of total strain

1) Compression test of composite

a) Sample Preparation: Standard cylindrical specimens of 12 mm X 12 mm Φ (H/D=1.0) and 12 mm X 18 mm Φ (H/D=1.5), were machined from the extruded material. Sample edges were chamfered to minimize folding. Concentric grooves of 0.5 mm depth were made on both the end surfaces of the sample.

b) Testing: A computer controlled servo hydraulic 100T (FIE-UTE Model) universal testing machine was used to upset the samples, figure 2.10. The machine and process details were given in tables 2.2 and 2.3 at chapter 2. Standard samples were upset by placing between the platens at a constant cross head speed in dry conditions. The compression tests were carried out until either 50% reduction in height or initiation of the fracture on the specimen surface whichever is earlier. A PC based data logging system was used to record and store the loads and displacements continuously.

The specimens subjected to upset forging, from 10% height reduction, with successive increments of 10%, to 50% height reduction or till the appearance of an appreciable crack whichever is earlier. A closer view of sample deformation was shown in figure 5.4. The image of specimens at various after deformation levels for Ho/Do = 1.0 and 1.5A

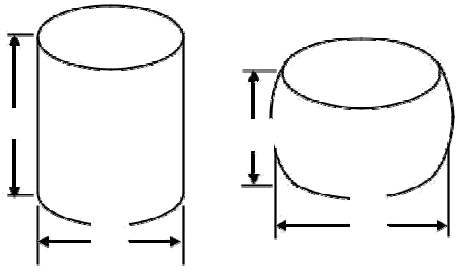

Schematic diagram of samples for upset tests

Image of specimen after 50% deformation (Ho/Do = 1.5) showing thebulge profile

Composite specimens showing bulge profiles at various deformation stages under compression testing (Ho/Do =1.0 & Ho/Do =1.5

V. RESULTS AND CONCLUTION.

The maximum radial displacement corresponding to 60% for the aspect ratio of 1.0 is shown as 2.435mm in figure 6.7. This means that the diameter after 60% deformation equals to 12 + 2 X 2.435 = 16.87 mm. The value of analytically determined diameter after 60% equals to 12 X = 16.970 mm, (assuming volume constancy) leading to a very little error of 069% usually can be discarded in non-linear finite element analysis such as in large deformation / metal forming applications.

For the present study the friction factor 'm' was found to be 0.38and the extent of barreling with this friction at 60% deformation for alloy and composites under investigation was shown in figures 3-6 respectively. Similar results on finding the friction were observed by many authors [11-28]. Lower aspect ratio (H0/D0 = 1.0) samples has shown more barreling affect compare to higher aspect ratio (H0/D0 = 1.5). The above results were experimentally evidenced, as discussed in chapter 5.

The notations used in the analysis were, radial displacements (UX): circumferential stress, (SY), axial stress z (SZ), hydrostatic stress, *H* (NLHPRE), Von-Mises equivalent stress (SEQV).

The variations in FEA results compared to analytical results obtained . The obtained FEA results revealed that these values are closely matching with the experimental values. Hence the FEA model adopted for solving the present upsetting analysis was validated with the analytical results of chapter 5.

A square shaped billet was taken and tested by applying the same material properties, and validated the results, as shown in figures .3-6, the platens were considered as rigid and due to symmetry, half portion was taken for analysis to reduce the problem size.

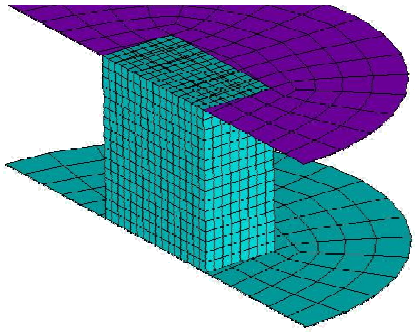

Figure 6.3 Half geometry after meshing, cylindrical shape (platens made rigid)

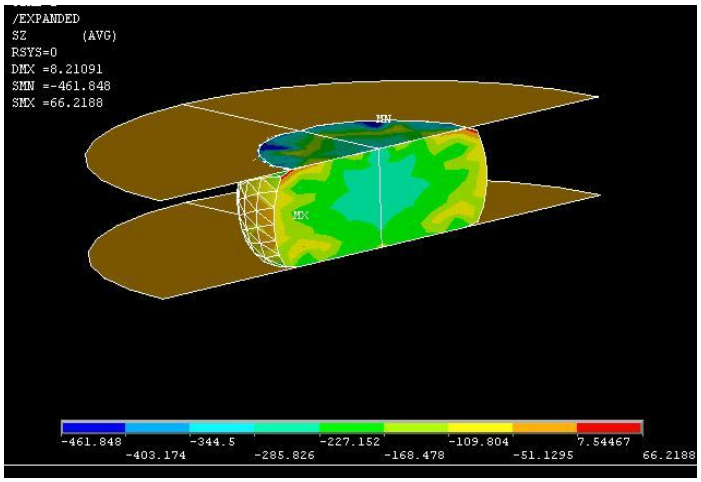

Figure .4 Half geometry after 60 % deformation (platens made rigid)(Circumferential stress)

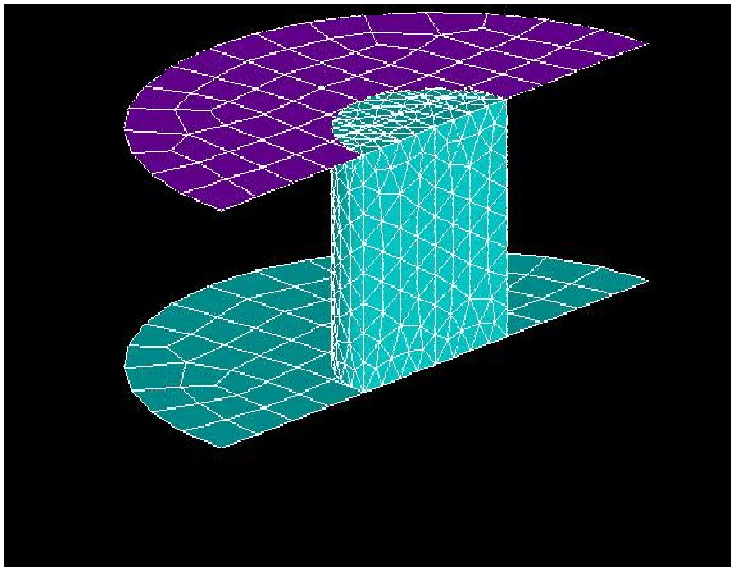

Figure 5 Half geometry after meshing, square shape (platens made rigid)

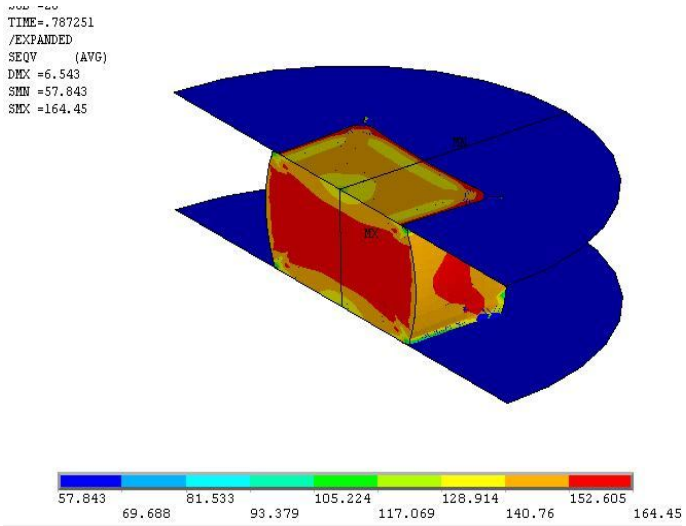

Figure 6 Square shaped specimen with half sectional view, after deformation (von-mises stress)

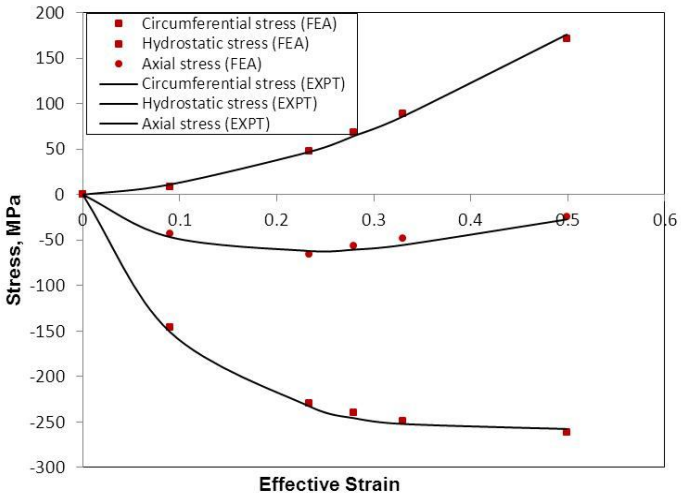

Graph

	C-K	O-K	Na-K	Mg-K	Al-K	Si-K	K-K	Ca-K	Ti-K	Mn-K	Fe-K	Cu-K	Zn-K
ARCI(793)_pt1	3.39	0.10	0.03	0.79	93.62	0.00	0.00	0.11	0.00	0.00	0.15	2.05	0.00
ARCI(793)_pt1	+/- 1.40	+/- 0.20	+/- 0.02	+/- 0.08	+/- 0.49	+/- 0.00	+/- 0.00	+/- 0.07	+/- 0.00	+/- 0.00	+/- 0.15	+/- 0.35	+/- 0.00

Figure EDS spectrum on the Flyash particulate

VI. CONCLUSIONS

1) The bulk density of the fly ash particles was found to be 2.52 g/cm3.
2) A6063/FA/SiC Hybrid composites were produced by stir casting route successfully.
3) There was a uniform distribution of FA/SiC particles in the matrix phase.
4) From the SEM figures, it clearly shows that there were no voids and discontinuities in the composites; there was a good interfacial bonding between the FA/SiC particles and matrix phase
5) The density of the composites decreases with increasing the percentages of FA/SiC particulates compared to the density of the alloy 2.780 g/cm3.
6) The measured densities were lower than that obtained from theoretical calculations. The extent of deviation increases with increasing FA/SiC content. From the EDX analysis of composites shows that no oxygen peaks were observed in the matrix area, confirming that the fabricated composite did not contain any additional contamination from the atmosphere.
7) The hardness of the composites increased with increasing the amount of FA/SiC than the base alloy.
8) Strength coefficient increases with increase in reinforcement content compared to the alloy.
9) At high aspect ratio both alloy and the composites exhibits lower compression strength values.
10) Strain hardening exponent increases with increase in reinforcement content compared the alloy.
11) At high aspect ratio, strength coefficient decreases while strain hardening exponent increases.
12) For both alloy and composites effective strain increases and the circumferential stress component becomes tensile with continued deformation.
13) The increase in circumferential stress component value was found to be more in case of specimens deformed for lower aspect ratio compared to the higher aspect ratio conditions
14) The axial stresses, for alloy as well as the composites increased in the very initial stages of deformation but started becoming less compressive immediately as barreling developed.

15) At the beginning of deformation axial compressive stress increased in magnitude but as the deformation progress the magnitude reduced.
16) Hydrostatic stress is reduced in magnitude as the deformation increased.
17) Meticulous comparisons of the experimental variables with the finite element method (FEM) results were carried out to ascertain the accuracy with which the deformation process can be modeled. Prediction from the simulation results were found to be in good agreement with the actual experimentation.
18) Finite element analysis of deformation behavior of cold upsetting process was carried out for all the composites and base alloy (A6063) with aspect ratios of 1.2 and 1.7 in dry condition.
19) Due to axisymmetric nature of the geometry only quarter portion was modeled with symmetric boundary conditions.
20) Rigid-flexible contact analysis was performed for the forming process, so that the die appears like a thin plate, and the stress analysis was done on the billet only.
21) FEM analysis, need material characteristics of composites. The stress strain curve obtained through UTM was only used for the analysis. The material models used in ansys helped in better correlation with results.
22) Once the material properties for composites and material model to be selected from ansys are finalized, the future designs that are going to be produced through these composites will require less time for manufacture.
23) The accuracy of results depends on the accuracy of the input data (true stress-true strain behavior and friction factor obtained from the experiments) and friction model used in the analysis.

S. No	Specimen	Density (g/cm^3)	
		Theoretical	Measured
1.	AA 6063alloy	2.9	2.95
2.	AA 6063alloy - 7% FA/SiC composite	3.1	2.65
3.	AA 6063alloy - 15% FA/SiC composite	2.2	2.54
4.	AA 6063alloy - 17% FA/SiC composite	2.3	2.20

REFERENCES

[1] R.K. Everett, and R.J.Arsenault, Metal Matrix Composites; Mechanisms and Properties, 1991 (Academic Press, San Diego).
[2] M.J. Kocjak, Kahtri S.C, J.E. Allison. Fundamentals of Metal Matrix Composites (Eds S. Suresh, A. Mortensen and A. Needleman), 1993 (Butterworth-Heinemann, Boston).
[3] Hassan S. F, Gupta, M, Development of high strength magnesium copper based hybrid composites with enhanced tensile properties, Materials Science andTechnology, 19 (2003) 253-259.
[4] Wu G.H., Dou Z. Y., Jiang L. T., Cao J. H., 2006, Damping properties of aluminium matrix – fly ash composites, Materials Letters, 60: 2945-2948.
[5] Davis Joseph R. ASM specialty hand book, aluminum and aluminum alloys. ASM International; 1993
[6] Mondolfo L. F., "Design Aluminium alloys: Structure and properties", Butterworth and Co (Publishers) Ltd. London, (1976) 253.
[7] BabuRao J. Syed Kamaluddin, AppaRao J., Sarcar M. M. M., Bhargava N.R.M.R., "Deformation behavior of Al–4Cu–2Mg alloy during cold upset forging", Journal of Alloys and Compounds, Vol. 471, 2009, pp. 128-136
[8] BabuRao J, VenkataRao D, Narasimha Murthy I., and Bhargava NRMR, "Mechanical properties and corrosion behaviour of fly ash particles reinforced AA 6061 composites", International Journal of Composite Materials (ISSN: 0021-9983)" –Vol.46(12), 2011, pp.1393-1404.

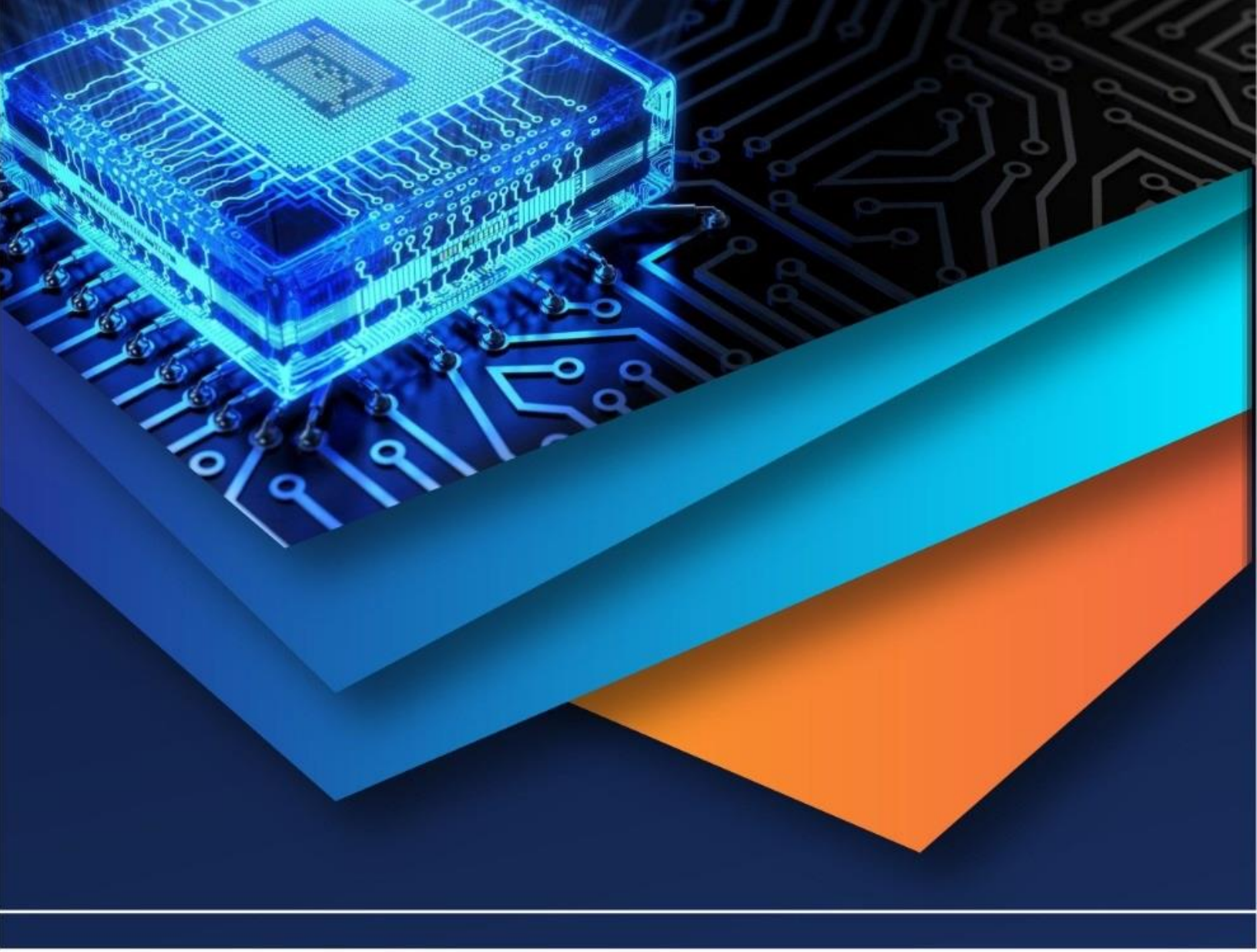

10.22214/IJRASET

45.98

IMPACT FACTOR: 7.129

IMPACT FACTOR: 7.429

INTERNATIONAL JOURNAL FOR RESEARCH

IN APPLIED SCIENCE & ENGINEERING TECHNOLOGY